TECHNICAL PAPER

CrossMark

Multi-objective optimization of parameters in turning of N-155 iron-nickel-base superalloy using gray relational analysis

Behzad Eskandari[1] · Behnam Davoodi[2] · Hamid Ghorbani[3]

Abstract

Obtaining high surface quality with minimum tool wear values is one of the most important goals of turning process. Moreover, when it comes to process costs, the volume of material removed is very important and should be considered when optimizing cutting variables. In this work, gray relational analysis was employed with the aim of simultaneously optimizing surface roughness, tool wear and volume of material removed. Cutting speed, feed rate and depth of cut were chosen as process control factors. Optimization results showed that cutting speed of 80 m/min, feed rate of 0.1 mm/rev and depth of cut of 1.5 mm were the optimum set of cutting parameters. Scanning electron microscope images of worn cutting edges revealed that depth-of-cut notch, built-up edge, and adhesion are dominant wear mechanisms. Finally, confirmation test proved the accuracy of the prediction carried out by the optimization process.

Keywords Iron-nickel-base superalloy · Turning · Gray relational analysis · Tool wear mechanism · Surface roughness · Volume of material removed

1 Introduction

Machining process which consists of removing of material and modification of part surface is a part of main manufacturing processes including casting, metal forming, powder metallurgy and joining processes. Parts manufactured by latter processes often need machining operations before using them. In other words, machining processes are often considered as secondary or finishing operations [1]. Turning process using single-point cutting tool is the most common used metal cutting operation [2]. A workpiece being machined by turning process is influenced by various force and temperature stresses, which, in turn, affect the final surface properties of the product. Achieving high accuracy and acceptable surface integrity including surface roughness, hardness, residual stresses, etc. during turning process is of primary importance. Surface integrity has significant effects on performance characteristics of the final product such as fatigue strength and creep [3]. Surface roughness is the most widely used surface integrity characteristic [4].

The effects of cutting parameters on surface roughness have been investigated by several researches. Meddour et al. [5] showed that the best surface roughness (Ra) was obtained using small feed rate and large nose radius. Arunachalam et al. [6] investigated the effects of cutting parameters on surface roughness and residual stress in machining of Inconel 718 nickel-base superalloy. According to their results, machining at low cutting speed and small depth of cut would lead to compressive or minimal tensile residual stresses and good surface finish. Zhou et al. [7] reported the effect of cutting parameters, tool wear and coolant condition on damage to the machined surface in finish turning of Inconel 718 with whisker-reinforced ceramic cutting tools. It was observed that the

Technical Editor: Márcio Bacci da Silva.

✉ Behnam Davoodi
bdavoodi@iust.ac.ir

Behzad Eskandari
beskandari89@ms.tabrizu.ac.ir

Hamid Ghorbani
hamid.ghorbani@polymtl.ca

1 Department of Manufacturing Engineering, Faculty of Mechanical Engineering, University of Tabriz, Tabriz, Iran

2 School of Mechanical Engineering, Iran University of Science and Technology, Tehran, Iran

3 Department of Mechanical Engineering, École Polytechnique de Montréal, Montréal, QC, Canada

type and extent of the surface damage were dependent upon the cutting parameters, the size of the wear land and the coolant conditions. Fernández-Valdivielso et al. [9] defined an inverse methodology to determine the best cutting tool features turning of Inconel 718 so as to reach the optimum surface integrity. Some scholars, on the other hand, have used soft computing to optimize surface roughness parameters. Sangwan et al. [8] used integrated ANN-GA approach to determine optimum cutting parameters to obtain the best surface roughness.

Cutting tools are subjected to force and temperature stresses which lead to tool wear. Various parameters affect tool wear rate and wear mechanisms such as cutting fluid [10], cutting speed and feed rate [11], as well as cutting material and geometry [12]. Furthermore, tool wear increases cutting forces [13] and as a result, worsens surface quality [14]. Seeman et al. [15] studied surface roughness and flank wear in turning of a kind of hard-to-machine composite material. In their research, it is shown that the formation of Built-up edge significantly affects the surface roughness at low speeds. Wear behavior of the cutting tool in cryogenic cooling was investigated by Wang et al. [16] in machining of GH4169 nickel-based superalloy. It was found that using liquid nitrogen as the cutting coolant, tool wear decreases at low and medium cutting speeds. Moreover, tool service life improves four times as better as that of the conventional machining.

Various methods have been used to optimize cutting parameters for improving tool life and achieving better surface quality such as Taguchi method. Zou et al. [17] used Taguchi L_9 orthogonal array to find optimum parameters of cutting speed and feed rate in turning of two kinds of stainless steel to improve surface roughness with the least tool wear. They showed that cutting speed was the most significant parameter on both materials. In addition, crater on the rake face and chipping were the dominant wear mechanisms. In the same way, Hasçalık and Çaydaş [18] used this method to optimize tool life and surface roughness. In this study, two separate optimum parameters were found for the response parameters. Another commonly used optimization method is response surface method (RSM). Dureja et al. [19] found optimal cutting parameters such as cutting speed, feed rate, depth of cut and material hardness to achieve minimum flank wear and surface roughness using RSM. Camposeco-Negrete [20] conducted a multi-objective optimization in which energy consumption and surface roughness were minimized, and material removal rate was maximized using RSM.

Gray relational analysis (GRA) is one of the effective approaches for the consideration of two or more response variables at the same time. This method was first proposed by Deng [21] and is widely used to estimate the behavior of an unknown system in which a multi-response problem is converted to a single-response one. By optimization of the new single-objective problem, the optimal combination of response parameters can be found. Previous researches have shown the effectiveness of this method for multi-objective optimizations. Pawade and Joshi [22] performed multi-objective optimization of surface roughness and cutting force components using Taguchi gray relational analysis (TGRA) in the high-speed turning of Inconel 718. It was confirmed that surface roughness was significantly improved at predicted optimum parameters. Angappan et al. [23] used Gray Taguchi-based analysis to optimize the machining parameters in turning of Incoloy superalloy without using cutting fluids. They showed that the combinational parameters (surface roughness, cutting force, and cutting power) were improved by 48.98%. According to the research conducted by Varghese et al. [24], a 77% improvement in GRG parameter was found when using Gray relational analysis method in the optimization of combination of cutting parameters in dry turning of 11SMn30 free cutting steel.

It is true that producing good surface roughness is desirable; however, it should be economically justifiable. In other words, to have better surface quality, the range of tool wear criteria should be limited so as to have less worn tool edges involved in the cutting process. Therefore, it would be better to have a trade-off between surface roughness, tool wear and volume of material removed per unit time.

In this work, gray relational analysis has been used for simultaneous consideration of tool wear, surface roughness and volume of material removed in turning of N-155 iron-nickel-based superalloy. Superalloys are classified as difficult-to-machine materials because they retain strength at high temperatures, contain hard carbides in their microstructures which make them abrasive, have high dynamic shear strength and work harden during metal cutting [25]. These properties exacerbate the difficulties concerning surface quality and tool wear which mentioned earlier. Iron-nickel-based superalloys possessing lower cost compared to other kinds of superalloys, namely nickel- and cobalt-based superalloys, are tough and ductile which suit them to be utilized in applications where these attributes are required, such as turbine discs and forged rotors. N-155 (multimet) is an iron-nickel-based superalloy which is only used in wrought condition [25] in gas turbines engine parts such as combustors, transition ducts, after-burners, as well as furnace hardware and industrial fans. Moreover, it is noteworthy that this material can be used in working temperatures up to 820 and 1090 °C for high and moderate stress applications, respectively.

2 Experimental procedure

Turning experiments were carried out on an Emcoturn 242 TC CNC lathe machine with the following specifications: maximum power 13 kW, spindle speed range 50–4500 rpm, feed range 0–4000 mm/min, Emcotronic TM 02 microprocessor-2-axis-Path control. PVD TiAlN-coated carbide inserts from Sandvik Company were used as the cutting tool material. The inserts ISO designation is CNMG 120404, and the grade of the coated carbide is designated by GC1105. Correspondingly, the inserts were mounted on a left-hand style tool holder coded PCBNL 2020M12. Average values of flank wear VB_a were measured after the 90s cutting time using a toolmakers microscope fitted with a digital camera and image analysis software. The procedure of selection of inserts and tool holder geometry and measurement of tool wear as well as the ranges of cutting parameters was done according to ISO 3685:1993 [26] and the manufacturer's handbook.

N-155 iron-nickel-base superalloy of 250 mm length and 34 mm diameter was used as the workpiece material. The chemical composition of the workpiece material is given in Table 1. The material was solution treated to a surface hardness around 32 HRc. Each machining experiment was carried out using a new cutting tool edge for 90s cutting time and under dry cutting condition. After each experiment, values of surface roughness, cutting tool wear, and volume of material removed were recorded.

Surface roughness parameter, Ra, which is arithmetic average of absolute roughness determined from deviations about the center line within the evaluation length [27], was considered as the surface roughness criteria of the turned surface. Surface roughness was measured by Mahr-perthometer M1 within the sampling length of 5.6 mm. The measurements of the surface roughness were repeated four times, and subsequently, Ra values were determined by averaging these values.

3 Multi-objective optimization using gray relational analysis (GRA)

Experiments were conducted according to Taguchi L_9 experimental design. Cutting speed (V), feed rate (f) and depth of cut (d) were selected as cutting parameters. With three control factors each in three levels (Table 2), according to Taguchi L_9 orthogonal array, there should be

Table 2 Experimental control factors and their levels

Control factors	Symbol	Level 1	Level 2	Level 3
Cutting speed (m/min)	V	80	100	120
Feed (mm/rev)	f	0.1	0.15	0.2
Depth of cut (mm)	d	0.5	1	1.5

9 experimental tests. Table 3 shows experimental design arrangement and the values of response variables, i.e. surface roughness (Ra), tool flank wear (VB_a) and volume of material removed (VMR). As mentioned earlier, in this study gray relational analysis (GRA) was used to determine optimum cutting parameters to achieve optimum response values. Gray relational analysis is utilized according to the following steps:

3.1 Step 1: data normalization

The first step in GRA is normalizing the experimental data between 0 and 1 for each response parameter to avoid the effect of adopting different units and reduce the variability. In this step, which is also called gray relational generating, three types of quality characteristics can be used; the-larger-the-better, the-nominal-the-better, the-smaller-the-better [21] (Eqs. 1–3). Depending on whether the response variable was to be minimized or maximized, one of the following quality characteristics was used for each response:

$$x_i^*(k) = \frac{x_i^0(k) - \min x_i^0(k)}{\max x_i^0(k) - \min x_i^0(k)}; \text{ the-larger-the-better} \quad (1)$$

$$x_i^*(k) = 1 - \frac{\left|x_i^0(k) - \text{OB}\right|}{\max[\max(x_i^0(k) - \text{OB}, \text{OB} - \min x_i^0(k))]};$$
$$\text{the-nominal-the-better} \quad (2)$$

$$x_i^*(k) = \frac{\max x_i^0(k) - x_i^0(k)}{\max x_i^0(k) - \min x_i^0(k)}; \text{the-smaller-the-better} \quad (3)$$

where $x_i^*(k)$ is the normalized value for $x_i^0(k)$ which is the kth dependent response of ith trial, OB is the target value and $\max x_i^0(k)$ and $\min x_i^0(k)$ are largest and smallest values of $x_i^0(k)$ for the kth response, respectively. Since higher amounts of volume of material removed were desirable, the-larger-the-better quality characteristic (Eq. 1) was used for VMR. On the other hand, our goal was to obtain minimum values of surface roughness and flank wear;

Table 1 Chemical composition of workpiece material

Chemical composition	Fe	Cr	Ni	Co	Mo	W	Nb	Mn	N	C	Zr
%wt	Balance	21.9	20.3	19.7	3	2.5	1	1.2	0.15	0.15	0.02

Table 3 Experimental design arrangement using L$_9$ Taguchi and the results

Experiment number	V (m/min)	f (mm/rev)	d (mm)	Ra (μm)	VB$_a$ (mm)	VMR (mm^3)
1	80	0.1	0.5	0.91	0.1	6091
2	80	0.15	1	1.65	0.13	18,562
3	80	0.2	1.5	2.03	0.23	37,748
4	100	0.1	1	0.84	0.14	15,468
5	100	0.15	1.5	1.65	0.17	35,383
6	100	0.2	0.5	1.83	0.3	15,226
7	120	0.1	1.5	1.26	0.2	29,070
8	120	0.15	0.5	1.57	0.17	13,704
9	120	0.2	1	3.14	0.33	37,124

hence, the-smaller-the-better quality characteristic (Eq. 3) was employed for these responses. Table 4 shows the normalized data after the application of respective equations. Basically, higher value of normalized experimental data indicates better performance and the best one should be equal to 1.

3.2 Step 2: calculation of gray relational coefficient (GRC)

After normalizing the experimental results, gray relational coefficients (GRC) were calculated using Eqs. (4) and (5):

$$\gamma_i(k) = \frac{\Delta_{\min} + \zeta \cdot \Delta_{\max}}{\Delta_{0i}(k) + \zeta \cdot \Delta_{\max}} \tag{4}$$

$$\Delta_{0i}(k) = \|x_0^*(k) - x_i^*(k)\| \tag{5}$$

where $\gamma_i(k)$ is GRC and ζ is the distinguishing coefficient varying from 0 to 1 which is generally determined as 0.5 [28]. $\Delta_{0i}(k)$ is the absolute value of the difference between reference sequence, $x_0^*(k) = 1$, and comparability sequence, $x_i^*(k)$ (Eq. 5). $\Delta_{\min}$ and $\Delta_{\max}$ are the smallest and the largest values of difference between $x_0^*(k)$ and $x_i^*(k)$ which are given by:

$$\Delta_{\min} = \min_{\forall j \in i} \left\| \min_{\forall k} x_0^*(k) - x_i^*(k) \right\| \tag{6}$$

$$\Delta_{\max} = \max_{\forall j \in i} \left\| \max_{\forall k} x_0^*(k) - x_i^*(k) \right\| \tag{7}$$

Gray relational coefficients denote the relationship between the ideal and the actual experimental results. The calculated values of GRCs are shown in Table 5.

3.3 Step 3: calculation of weighted gray relational grade (WGRG)

Gray relational grade (GRG) is calculated by averaging the gray relational coefficient values of each performance characteristic, and it is defined as:

$$\gamma_i = \frac{1}{m} \sum_{k=1}^{m} \gamma_i(k) \tag{8}$$

where γ_i is GRG for ith experiment and m is the number of response variables. Influence of each response parameter can be established through assigning weight factors for each one. Weighted gray relational grades (WGRG) are computed as follows:

Table 4 Normalized values

Trial no.	Ra (μm)	VB$_a$ (mm)	VMR (mm^3)
1	0.96956522	1	0
2	0.64782609	0.86956522	0.39394131
3	0.4826087	0.43478261	1
4	1	0.82608696	0.29620621
5	0.64782609	0.69565217	0.92529298
6	0.56956522	0.13043478	0.28856177
7	0.8173913	0.56521739	0.72587421
8	0.6826087	0.69565217	0.24048394
9	0	0	0.98028872

Table 5 Calculated values of GRC

Trial no.	Ra (μm)	VB$_a$ (mm)	VMR (mm^3)
1	0.942623	1	0.333333
2	0.586735	0.793103	0.452056
3	0.491453	0.469388	1
4	1	0.741935	0.415354
5	0.586735	0.621622	0.870009
6	0.537383	0.365079	0.412733
7	0.732484	0.534884	0.64589
8	0.611702	0.621622	0.396978
9	0.333333	0.333333	0.962073

Table 6 Mean values of GRC

	Ra (μm)			VB$_a$ (mm)			VMR (mm^3)		
	Feed	Vc	Doc	Feed	Vc	Doc	Feed	Vc	Doc
Level 1	0.891	0.673	0.697	0.758	0.754	0.662	0.464	0.595	0.381
Level 2	0.595	0.708	0.64	0.678	0.576	0.622	0.573	0.566	0.609
Level 3	0.454	0.559	0.603	0.389	0.496	0.541	0.791	0.668	0.838
Range (max–min)	0.437	0.114	0.093	0.369	0.257	0.120	0.326	0.102	0.457
ΣRange	0.645			0.747			0.886		
Weight	0.285			0.33			0.39		

$$\gamma_{wi} = \frac{1}{m} \sum_{k=1}^{m} w_k \gamma_i(k) \quad (9)$$

where γ_{wi} is WGRG and w_k is weight factor for each response variable sum of which is equal to 1.

Assigning appropriate weight factor values for each response has great significance. In many researches, equal weight is used to determine the WGRGs [29], whereas some other researchers have selected different values for each response to increase or decrease the influence of each one on the optimal results [30]. As Yan and Li [31] explained these methods are not reasonable approach regarding determining appropriate weight factors. In this study, the influence degree of input parameters' variations on each response is proposed to establish response weight factors. In other words, weight factors have been considered to be dependent on the influence rate of cutting conditions' variations on response parameters. Therefore, the weight factor of responses were large when the cutting parameters' variations have the high influence on each response and vice versa.

To do so, first mean values of GRC and then the variations' range of it (max–min) were calculated for each level of each response parameter. The GRC range is determined as:

$$R_{i,j} = \max\{K_{i,j,1}, K_{i,j,2}, \cdots K_{i,j,k}\}$$
$$- \min\{K_{i,j,1}, K_{i,j,2}, \cdots K_{i,j,k}\}; \begin{cases} i = 1, 2\ldots m \\ j = 1, 2\ldots p \\ k = 1, 2\ldots l \end{cases} \quad (10)$$

where R is the GRC range and m, p and l are the number of responses, number of cutting parameters and number of experimental levels, respectively. In this study, values of p, m, and l are 3. In addition, K is the average GRC for each cutting parameter's level at each response. The larger amount of R indicates that the influence degree of input parameters' change on each response is larger. Thus, the weight factor for each response (w) is determined as follows:

$$w_i = \frac{\sum_{j=1}^{p} R_{i,j}}{\sum_{i=1}^{m} \sum_{j=1}^{p} R_{i,j}} \quad (11)$$

In Table 6 mean values of GRC for each level of response parameters are summarized. In the fourth row of this table the values of $R_{i,j}$ for ith response and jth cutting parameter is depicted. The next row shows the sum of the GRC range for each response ($\sum_{j=1}^{3} R_{i,j}$). By dividing this value by sum of the GRC range values of three responses ($\sum_{i=1}^{3} \sum_{j=1}^{3} R_{i,j}$), weight factor value for each response is determined (last low). According to the results, for each experiment WGRG values are expressed as:

$$\text{WGRG} = 0.28\text{GRC}_{\text{Ra}} + 0.33\text{GRC}_{\text{VB}} + 0.39\text{GRC}_{\text{VMR}} \quad (12)$$

where GRC_{Ra}, GRC_{VB} and GRC_{VMR} are GRC values of surface roughness, tool wear and volume of material removed, respectively. The calculated WGRC values of responses are given in Table 7 in the descending order. Thus, experiment number 1 is the best combination of cutting parameters in terms of WGRG.

3.4 Step 4: optimization of response parameters

Through the steps of 1–3, three response parameters, namely surface roughness, flank wear and volume of material removed were converted to a single-response

Table 7 The calculated WGRC

Experiment number	WGRG	Order
1	0.724	1
2	0.602	6
3	0.681	4
4	0.688	3
5	0.708	2
6	0.432	9
7	0.634	5
8	0.531	8
9	0.577	7

Table 8 Average WGRG for each input parameters

Cutting parameters	Average WGRG			Max–min	Rank
	Level 1	Level 2	Level 3		
Cutting speed (m/min)	**0.669**	0.609	0.581	0.088	3
Feed rate (mm/rev)	**0.682**	0.613	0.564	0.118	1
Depth of cut (mm)	0.562	0.622	**0.674**	0.112	2

The bold values are the optimum cutting parameters (green spots in the Fig. 1)

Fig. 1 Weighted gray relational grade (WGRG) graph
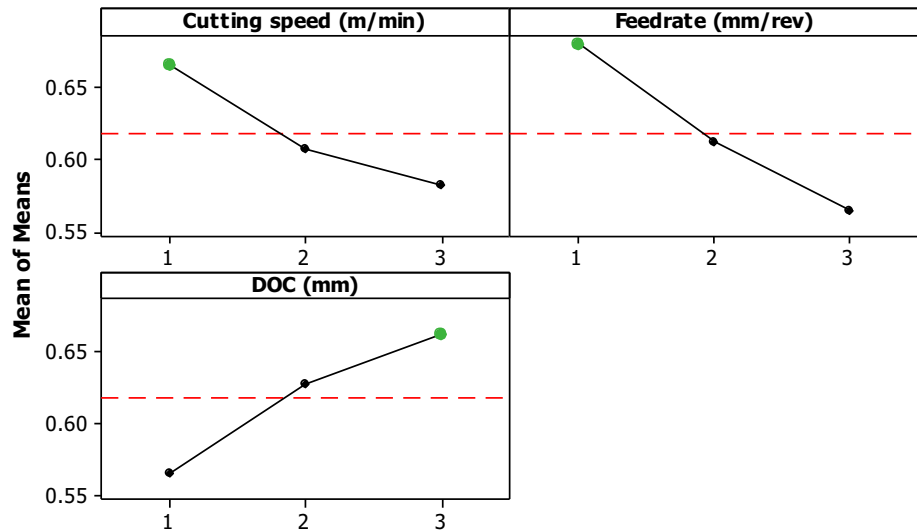
Table 9 ANOVA results for WGRG

Factors	Degree of freedom	Sum of squares	Mean squares	F ratio $\alpha = 5\%$	P value
Cutting speed	2	0.01221	0.00611	0.60	0.662
Feed rate	2	0.02109	0.01054	1.04	0.518
Depth of cut	2	0.01885	0.00942	0.93	0.598
Error	2	0.02037	0.01018		
Total	8	0.07252			

factor, i.e. WGRG, which was considered as the only response parameter for the rest of the analysis. By calculating the average values of WGRG corresponding to each level of the parameters, the best level of cutting parameters were identified, as are presented in Table 8 and Fig. 1.

According to the results, higher values of WGRG were obtained at the first level of cutting speed, 80 m/min, the first level of feed rate, 0.1 mm/rev, and third level of depth of cut, 0.5 mm.

Table 10 Results of calculated values of WGRGs for initial and optimum parameters

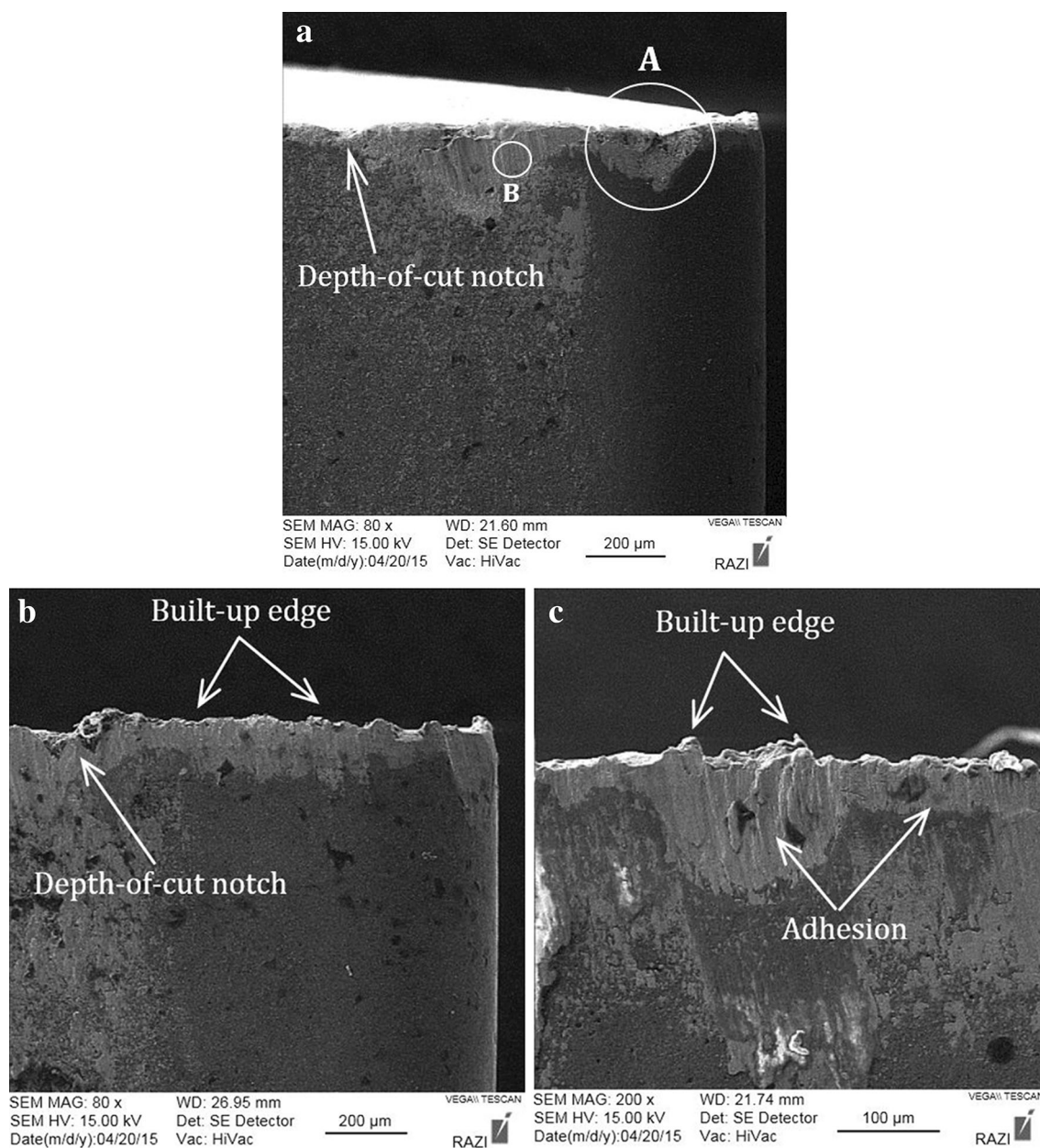|	Initial machining parameter	Optimal machining parameter	
		Prediction	Experiment
Level	$V_3f_3d_2$	$V_1f_1d_3$	$V_1f_1d_3$
Ra (μm)	3.14		0.89
VB$_a$ (mm)	0.33		0.10
VMR (mm^3)	37,124		18,870
WGRG	0.577	0.786	
Improvement in WGRG		0.209	

Fig. 2 SEM images of tool flank face at experimental set based on Table 3 **a** trial no. 1, **b** trial no. 2, **c** trial no. 3

3.5 Step 5: analysis of variance (ANOVA) for WGRG

To determine the significant parameters and the percentage contribution of each parameter on responses, analysis of variance (ANOVA) was carried out. Confidence level and significance of ANOVA analysis is 95 and 5%, respectively. Table 9 shows the results of ANOVA for the weighted gray relational grade. F values indicates the significance of control factors. According to this table, feed rate and cutting speed with the F values of 1.04 and 0.6 are the most and the least influential variables, respectively;

however, it is observed that none of the cutting parameters are statistically significant.

3.6 Step 6: prediction of WGRG under optimum parameters

Once the optimal combination of cutting parameters is predicted, the next step in GRA is to predict and confirm the improvement of multiple quality characteristics at the optimal level of cutting parameters via performing the confirmation test. The estimated optimum WGRG (γ_{opt}) is expressed as:
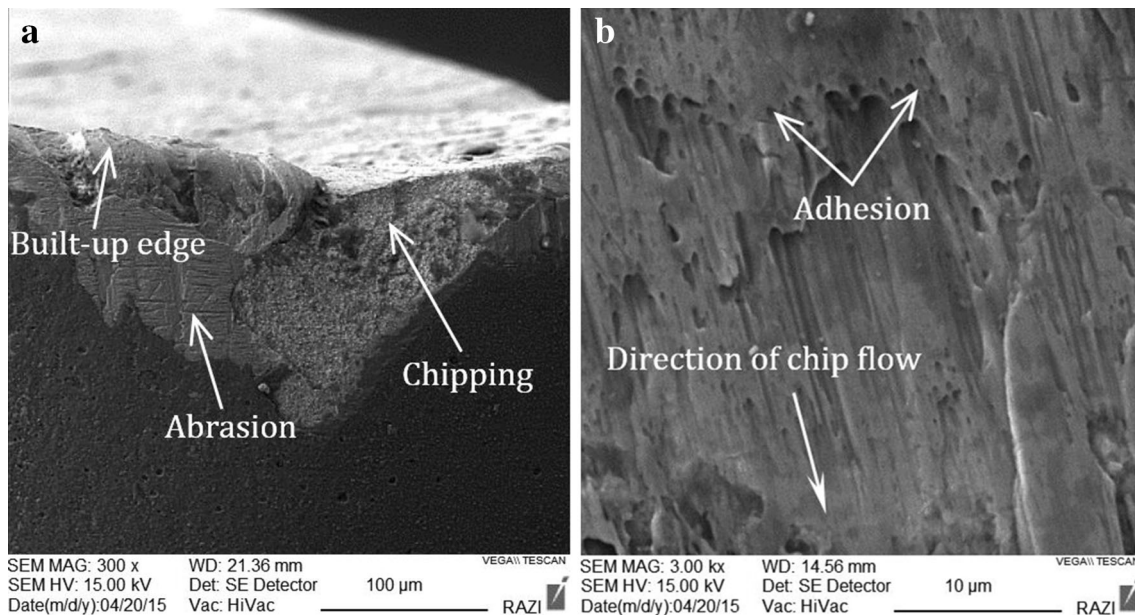
Fig. 3 Detailed image of **a** zone A, and **b** zone B, of Fig. 2a

$$\gamma_{\text{opt}} = \gamma_m + \sum_{i=1}^{n} (\gamma_i - \gamma_m) \qquad (13)$$

where γ_m is the total mean of the WGRG, γ_i is the mean WGRG at optimal level, and n is the number of the main design parameters which significantly affect the quality characteristics. The results of the confirmation experiment are presented in Table 10. As shown in the table, it is observed that WGRG of confirmation test is improved by 0.209.

4 Cutting tool wear analysis

In view of the importance of cutting tool wear in relation to the final surface quality and machining costs, in this section tool wear mechanisms are elaborated. Figures 2, 3, 4 and 5 show the scanning electron microscope (SEM) images of cutting tool flank wear at 80, 100 and 120 m/min cutting speeds, respectively. According to Fig. 1, the first level of cutting speed leads to the best overall results. As can be seen in Fig. 2, at 80 m/min cutting speed, the width of flank wear is low with slight depth-of-cut notch, and built-up edge (BUE) formed at the cutting edge. Depth-of-cut notch is resulted from intermittent cutting contact between tool and workpiece material on the rake face which continues down to the flank face causing accelerated wear in these regions. Abrasion and metal transfer are the most important factors contributing to notching wear [2]. Detailed image of cutting edge of Fig. 2a shown in Fig. 3a illustrates the presence of slight chipping and abrasion

wearing as well. Abrasion is the result of hard particles and impurities existing within the workpiece material [32].

Another mechanism which dominates throughout this research is adhesion. Formation of adhering layers on the flank face of the cutting tool is attributed to bonding between the newly generated surface of workpiece and tool flank face. Two factors mostly contributing to promote metallic bonding at tool/workpiece interface are considered to be plastic deformation and the absence of contamination. During turning process flow of material across the cutting tool is unidirectional (Fig. 3b), as a result, contaminants such as oxide films and lubricants are swept away resulting in prepared condition for adhesion [2]. Adhering layers on the flank face shown in Fig. 2a is illustrated in detail in Fig. 3b. Quantitative data of energy-dispersive X-ray spectroscopy (EDS) of this zone is presented in Table 11. The values of atomic percentage of iron and nickel confirmed that workpiece material was attached to the tool flank face and caused adhesion wear. These results of EDS analysis were observed in almost all the wear zones of this study.

Figure 4 shows the wear mechanisms occurred at 100 m/min cutting speed. Larger depth-of-cut notch and built-up edge are observable. Built-up edge is accumulated strain-hardened work material which alters tool edge geometry [33]. By formation of BUE, shear plane, in which intense shear strains occur during metal cutting, transfers from tool edge to top of the BUE. Amount of adhered layer attached to the tool flank face is also larger in comparison to the one at 80 m/min cutting speed.
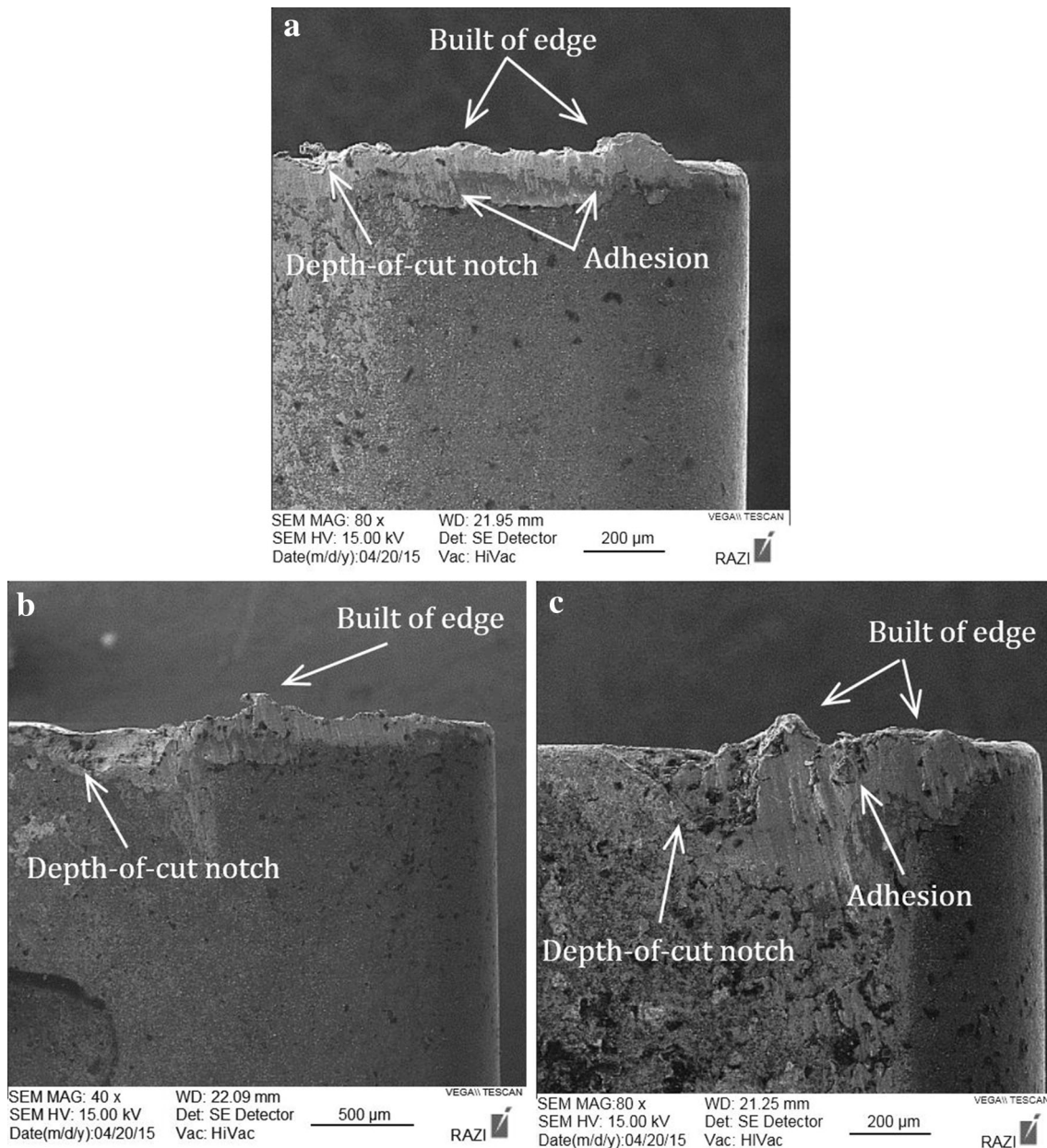
Fig. 4 SEM images of tool flank face at experimental set based on Table 3 **a** trial no. 4, **b** trial no. 5, **c** trial no. 6

At 120 m/min cutting speed, there are large built-up edge and depth-of-cut notch on the cutting tools (Fig. 5). Moreover, in Fig. 5c a large amount of chipping can be observed. One possible reason can be the constant formation of the built-up edge which is broken away resulting from lack of rigidity of machine tool at high cutting speed and feed rates [2], which consequently leads to the worst surface roughness (Fig. 6).

According to Fig. 1 by increasing in feed rate, overall quality characteristics deteriorate. Figures 2, 3, 4 and 5 confirm that increase in feed rate results in more wear rate and larger wear mechanisms at constant cutting speed. This can be explained that increase in feed rate results in more heat generation during metal cutting due to higher thermal loading and larger uncut chip thickness leading to increased impressive cutting forces on the cutting insert [34] and less tool life [35].

5 Conclusions

This research tried to investigate the optimization of one of the most important alloys from different aspects involved in turning process, i.e., workpiece, cutting tool and
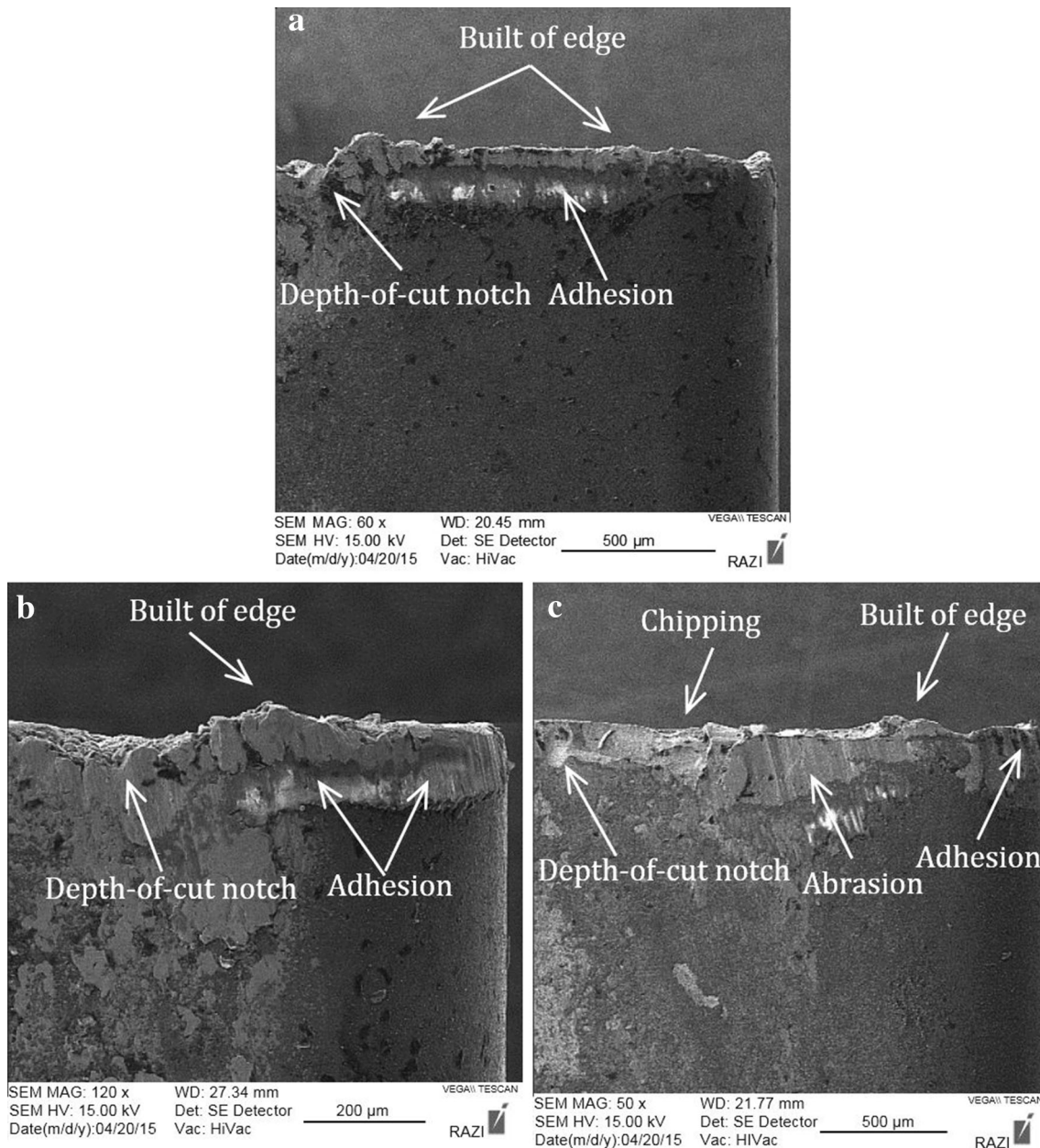
Fig. 5 SEM images of tool flank face at experimental set based on Table 3 **a** trial no. 7, **b** trial no. 8, **c** trial no. 9

machining economics. For this purpose, surface roughness, flank wear, and volume of material removed were investigated in turning of N-155 iron-nickel-base superalloy. Gray relational analysis was utilized so as to evaluate the effect of cutting speed, feed rate and depth of cut on the response parameters. Multi-objective optimization was carried out to determine minimum values of surface roughness and flank wear with the maximum amount of material removed. In addition, scanning electron microscope images of tool flank faces were used to closely examine the flank wear mechanisms. According to the experiments and subsequently performed analyses, following conclusions can be drawn:

- Cutting parameter set of $V_1 f_1 d_3$, i.e., 80 m/min cutting speed, 0.1 mm/rev feed rate, and 0.5 mm depth of cut, was determined to be the optimum machining variables.
- Confirmation of improvement of 0.209 in WGRG value proved the accuracy of optimum parameters predicted by GRA.
- SEM images showed that depth-of-cut notch, built-up edge, and adhesion were tool wear mechanisms which significantly affected the cutting tool.

Table 11 Quantitative data of EDS analysis of zone B in Fig. 2a

Element	Series	Atomic %
Silicon	K series	3.95
Chromium	K series	20.68
Manganese	K series	1.45
Iron	K series	31.33
Cobalt	K series	20.81
Nickel	K series	19.25
Molybdenum	L series	2.53
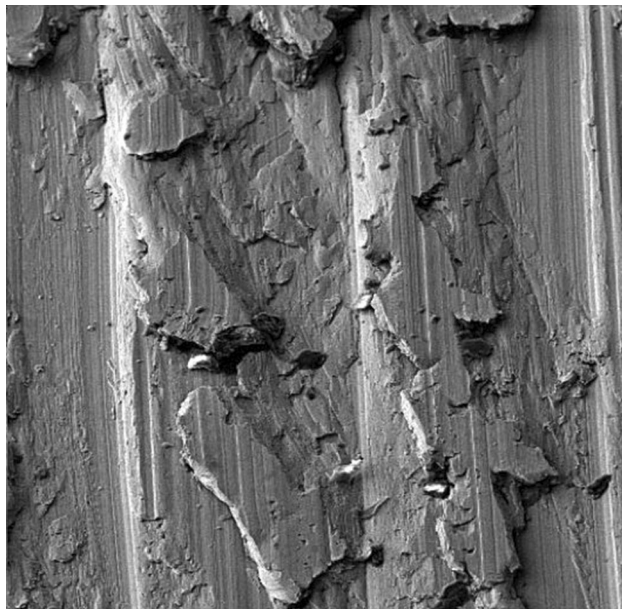
Fig. 6 SEM image of workpiece surface obtained at experimental set based on Table 3 trial no. 9

- Machining economics has been neglected by most of the researchers; however, in practice, it is one of the most decisive factors in selecting the preferred cutting parameters. This work considered one of its factors (volume of material removed). However, in the future works, other parameters such as cutting time and tooling costs, as well as other cutting factors such as surface hardness and cutting forces can be incorporated in the optimization of these alloys so that more accurate evaluation of machinability of these alloys will be achieved.

References

1. Kalpakjian S (2001) Manufacturing engineering and technology. Pearson Education India, Delhi
2. Trent EM, Wright PK (2000) Metal cutting. Butterworth-Heinemann, Boston
3. Bailey J, Jeelani S, Becker S (1976) Surface integrity in machining AISI 4340 steel. J Manuf Sci Eng 98(3):999–1006
4. Devillez A, Le Coz G, Dominiak S, Dudzinski D (2011) Dry machining of Inconel 718, workpiece surface integrity. J Mater Process Technol 211(10):1590–1598
5. Meddour I, Yallese M, Khattabi R, Elbah M, Boulanouar L (2015) Investigation and modeling of cutting forces and surface roughness when hard turning of AISI 52100 steel with mixed ceramic tool: cutting conditions optimization. Int J Adv Manuf Technol 77(5–8):1387–1399
6. Arunachalam R, Mannan M, Spowage A (2004) Residual stress and surface roughness when facing age hardened Inconel 718 with CBN and ceramic cutting tools. Int J Mach Tools Manuf 44(9):879–887
7. Zhou J, Bushlya V, Stahl J (2012) An investigation of surface damage in the high speed turning of Inconel 718 with use of whisker reinforced ceramic tools. J Mater Process Technol 212(2):372–384
8. Sangwan KS, Saxena S, Kant G (2015) Optimization of machining parameters to minimize surface roughness using integrated ANN-GA approach. Proc CIRP 29:305–310
9. Fernández-Valdivielso A, López de Lacalle L, Urbikain G, Rodriguez A (2016) Detecting the key geometrical features and grades of carbide inserts for the turning of nickel-based alloys concerning surface integrity. Proc Inst Mech Eng Part C J Mech Eng Sci 230(20):3725–3742
10. Lawal S, Choudhury I, Nukman Y (2015) Experimental evaluation and optimization of flank wear during turning of AISI 4340 steel with coated carbide inserts using different cutting fluids. J Inst Eng (India) Ser C 96(1):21–28
11. Davoodi B, Eskandari B (2015) Tool wear mechanisms and multi-response optimization of tool life and volume of material removed in turning of N-155 iron–nickel-base superalloy using RSM. Measurement 68:286–294
12. Jawaid A, Koksal S, Sharif S (2001) Cutting performance and wear characteristics of PVD coated and uncoated carbide tools in face milling Inconel 718 aerospace alloy. J Mater Process Technol 116(1):2–9
13. Chinchanikar S, Choudhury S (2016) Cutting force modeling considering tool wear effect during turning of hardened AISI 4340 alloy steel using multi-layer TiCN/Al2O3/TiN-coated carbide tools. Int J Adv Manuf Technol 83:1749–1762
14. Xue C, Chen W (2011) Adhering layer formation and its effect on the wear of coated carbide tools during turning of a nickel-based alloy. Wear 270(11):895–902
15. Seeman M, Ganesan G, Karthikeyan R, Velayudham A (2010) Study on tool wear and surface roughness in machining of particulate aluminum metal matrix composite-response surface methodology approach. Int J Adv Manuf Technol 48(5–8):613–624
16. Wang F, Li L, Liu J, Shu Q (2017) Research on tool wear of milling nickel-based superalloy in cryogenic. Int J Adv Manuf Technol 91(9–12):3877–3886
17. Zou B, Zhou H, Huang C, Xu K, Wang J (2015) Tool damage and machined-surface quality using hot-pressed sintering Ti (C7N3)/WC/TaC cermet cutting inserts for high-speed turning stainless steels. Int J Adv Manuf Technol 79(1–4):197–210

18. Hasçalık A, Çaydaş U (2008) Optimization of turning parameters for surface roughness and tool life based on the Taguchi method. Int J Adv Manuf Technol 38(9–10):896–903

19. Dureja J, Gupta V, Sharma VS, Dogra M (2009) Design optimization of cutting conditions and analysis of their effect on tool wear and surface roughness during hard turning of AISI-H11 steel with a coated—mixed ceramic tool. Proc Inst Mech Eng Part B J Eng Manuf 223(11):1441–1453

20. Camposeco-Negrete C (2015) Optimization of cutting parameters using response surface method for minimizing energy consumption and maximizing cutting quality in turning of AISI 6061 T6 aluminum. J Clean Prod 91:109–117

21. Deng J-L (1989) Introduction to grey system theory. J Grey Syst 1(1):1–24

22. Pawade RS, Joshi SS (2011) Multi-objective optimization of surface roughness and cutting forces in high-speed turning of Inconel 718 using Taguchi grey relational analysis (TGRA). Int J Adv Manuf Technol 56(1–4):47–62

23. Angappan P, Thangiah S, Subbarayan S (2017) Taguchi-based grey relational analysis for modeling and optimizing machining parameters through dry turning of Incoloy 800H. J Mech Sci Technol 31(9):4159–4165

24. Varghese L, Aravind S, Shunmugesh K (2017) Multi-objective optimization of machining parameters during dry turning of 11SMn30 free cutting steel using grey relational analysis. Mater Today Proc 4(2):4196–4203

25. Donachie MJ (2002) Superalloys: a technical guide. ASM International, Ohio, USA

26. International Standard ISO 3685, Tool-life testing with single-point turning tools, Edition ed., 1993-11-15

27. Griffiths B (2001) Manufacturing surface technology: surface integrity and functional performance. Butterworth-Heinemann, Boston

28. Sarıkaya M, Güllü A (2015) Multi-response optimization of minimum quantity lubrication parameters using Taguchi-based grey relational analysis in turning of difficult-to-cut alloy Haynes 25. J Clean Prod 91:347–357

29. Kuram E, Ozcelik B (2013) Multi-objective optimization using Taguchi based grey relational analysis for micro-milling of Al 7075 material with ball nose end mill. Measurement 46(6):1849–1864

30. Senthilkumar N, Tamizharasan T, Anandakrishnan V (2014) Experimental investigation and performance analysis of cemented carbide inserts of different geometries using Taguchi based grey relational analysis. Measurement 58:520–536

31. Yan J, Li L (2013) Multi-objective optimization of milling parameters–the trade-offs between energy, production rate and cutting quality. J Clean Prod 52:462–471

32. Ezugwu E, Wang Z, Machado A (1999) The machinability of nickel-based alloys: a review. J Mater Process Technol 86(1):1–16

33. Rollason E, Williams J (1970) Metallurgical and practical machining parameters affecting built-up-edge formation in metal cutting. J Inst Met 98:144–153

34. Ghorbani H, Moetakef-Imani B (2016) Specific cutting force and cutting condition interaction modeling for round insert face milling operation. Int J Adv Manuf Technol 84:1705–1715

35. Khan S, Soo S, Aspinwall D, Sage C, Harden P, Fleming M, White A, M'Saoubi R (2012) Tool wear/life evaluation when finish turning Inconel 718 using PCBN tooling. Proc CIRP 1:283–288